

BRIEF DEFINITIVE REPORT

Cell-intrinsic adrenergic signaling controls the adaptive NK cell response to viral infection

Carlos Diaz-Salazar^{1,2} , Regina Bou-Puerto^{1,2}, Adriana M. Mujal¹, Colleen M. Lau¹, Madlaina von Hoesslin³ , Dietmar Zehn³, and Joseph C. Sun^{1,2,4} 

Natural killer (NK) cells are innate lymphocytes that exhibit adaptive features, such as clonal expansion and memory, during viral infection. Although activating receptor engagement and proinflammatory cytokines are required to drive NK cell clonal expansion, additional stimulatory signals controlling their proliferation remain to be discovered. Here, we describe one such signal that is provided by the adrenergic nervous system, and demonstrate that cell-intrinsic adrenergic signaling is required for optimal adaptive NK cell responses. Early during mouse cytomegalovirus (MCMV) infection, NK cells up-regulated *Adrb2* (which encodes the β_2 -adrenergic receptor), a process dependent on IL-12 and STAT4 signaling. NK cell-specific deletion of *Adrb2* resulted in impaired NK cell expansion and memory during MCMV challenge, in part due to a diminished proliferative capacity. As a result, NK cell-intrinsic adrenergic signaling was required for protection against MCMV. Taken together, we propose a novel role for the adrenergic nervous system in regulating circulating lymphocyte responses to viral infection.

Introduction

Natural killer (NK) cells are innate lymphocytes with the ability to kill virally infected, stressed, or transformed cells through the recognition of ligands normally absent in healthy cells, or detection of missing ligands normally present (Lanier, 2008; Yokoyama et al., 2004). Because they express germline-encoded receptors and do not undergo antigen receptor rearrangement, NK cells have traditionally been categorized as a component of the innate immune system. Nonetheless, recent evidence suggests that NK cells exhibit adaptive features during their response against pathogens (Geary and Sun, 2017; Sun and Lanier, 2011; Vivier et al., 2011). Following viral infection in humans, nonhuman primates, and mice, subsets of NK cells have been described to undergo a clonal-like expansion and form a pool of long-lived memory-like cells (Daniels et al., 2001; Dokun et al., 2001; Gumá et al., 2004; Lopez-Vergès et al., 2011; Reeves et al., 2015; Sun et al., 2009). During mouse cytomegalovirus (MCMV) infection, adaptive NK cell responses are triggered through the engagement of the activating receptor Ly49H, expressed by a subset of NK cells, with the virally encoded glycoprotein m157, expressed on infected cells (Arase et al., 2002; Sun et al., 2009). In addition to this receptor–ligand engagement, Ly49H⁺ NK cells require pro-inflammatory cytokine signals to drive clonal expansion and memory formation (Geary et al., 2018; Madera et al., 2016; Madera and Sun, 2015; Sun et al., 2012). However,

the contribution of additional signals driving these adaptive features in NK cells during viral infection remains to be elucidated.

It is now becoming clear that catecholamines released by the adrenergic nervous system (ANS), such as epinephrine and norepinephrine, play a prominent role in regulating innate immune responses to pathogens such as bacteria and helminths (Godinho-Silva et al., 2019; Klose and Artis, 2019; Quatrini et al., 2018a). Stimulation of the β_2 adrenergic receptor (β_2 AR) on tissue-resident immune cells (e.g., macrophages and innate lymphoid cells) by adrenergic neurons results in reduced barrier inflammatory responses during various infectious settings (Gabanyi et al., 2016; Moriyama et al., 2018). Whether β_2 AR signaling directly impacts circulating lymphocytes, however, has not been clearly addressed. Although global effects of epinephrine on NK cell circulation and function have been described for a variety of settings (Bigler et al., 2015; Breen et al., 2016; Liu et al., 2017; Tarr et al., 2012), the direct cross-talk between the ANS and NK cells during viral infection has not been carefully investigated. In this study, we sought to determine whether adrenergic signaling plays a role in modulating the NK cell response to viral infection, and to elucidate the mechanisms underlying such regulation.

¹Immunology Program, Memorial Sloan Kettering Cancer Center, New York, NY; ²Department of Immunology and Microbial Pathogenesis, Weill Cornell Medical College, New York, NY; ³Division of Animal Physiology and Immunology, Technical University of Munich, Freising, Germany; ⁴Louis V. Gerstner, Jr. Graduate School of Biomedical Sciences, Memorial Sloan Kettering Cancer Center, New York, NY.

Correspondence to Joseph C. Sun: sunj@mskcc.org.

© 2020 Diaz-Salazar et al. This article is distributed under the terms of an Attribution–Noncommercial–Share Alike–No Mirror Sites license for the first six months after the publication date (see <http://www.rupress.org/terms/>). After six months it is available under a Creative Commons License (Attribution–Noncommercial–Share Alike 4.0 International license, as described at <https://creativecommons.org/licenses/by-nc-sa/4.0/>).

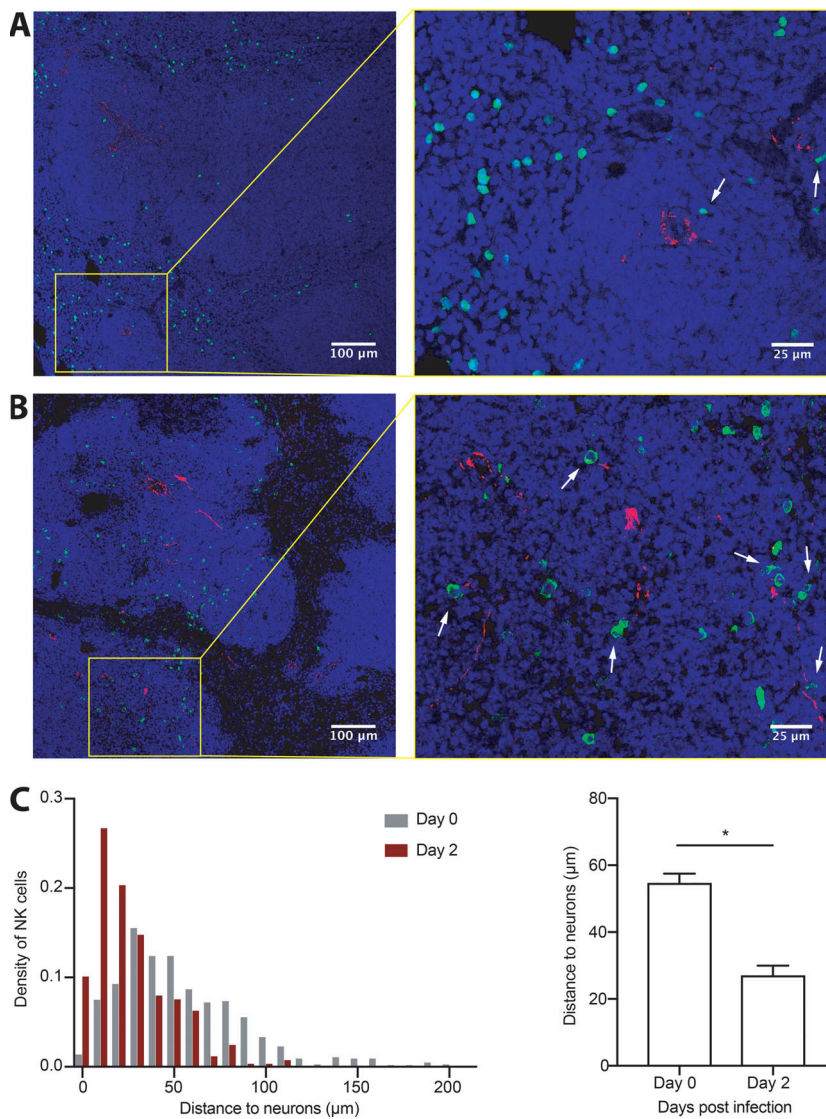


Figure 1. NK cells migrate to areas rich in adrenergic innervation during their response to viral infection. (A and B) Representative sections of spleen from WT mice showing NK cells (green), TH (red), and DAPI nuclear staining (blue) at steady-state (A), or 2 d following MCMV infection (B). White arrows indicate NK cells in close proximity to adrenergic fibrils. **(C)** Graphs show density distribution of the distances between NK cells and neurons at day 0 versus 2 PI (left) and quantification of the average distance (right). Data are representative of two independent experiments with two spleens per condition. Quantification was performed on representative images of equal area and comparable distribution of white and red pulp. Statistical differences ($P < 0.05$) are indicated with a single star (*) and were calculated with a nonparametric Mann-Whitney U test. All bar plots show mean \pm SEM.

Results and discussion

NK cells localize near splenic adrenergic neurons during viral infection

Secondary lymphoid organs are heavily innervated by the ANS. In the spleen, most sympathetic nerve fibers, characterized by tyrosine hydroxylase (TH⁺) expression, are located in the white pulp, particularly surrounding central arteries (Murray et al., 2017; Rosas-Ballina et al., 2008). Since interactions between TH⁺ fibers and lymphocytes in the spleen have been shown to be involved in coordinating immune responses to multiple infectious and noninfectious insults (Murray et al., 2017; Prass et al., 2003), we investigated the dynamics of NK cell trafficking in the spleen during viral infection and their relative proximity to splenic adrenergic neurons. Consistent with previous reports (Andrews et al., 2001; Bekiaris et al., 2008; Grégoire et al., 2008), we observed that most NK cells reside in the red pulp area of the spleen at steady-state, resulting in a spatial separation between adrenergic nerve fibers and NK cells (Fig. 1 A). However, during MCMV infection, NK cells trafficked into the white pulp (Fig. 1 B), a process thought to be regulated by pro-

inflammatory chemokines (Grégoire et al., 2008). Consequently, NK cells were found in closer proximity to TH⁺ fibers at day 2 post-infection (PI), with the median NK cell–neuron distance decreasing by more than twofold (Fig. 1 C).

NK cells up-regulate *Adrb2* during viral infection in an IL-12- and STAT4-dependent manner

We next determined whether NK cells possessed the cell-intrinsic ability to directly receive neuron-derived adrenergic signals. Among the nine known adrenoceptor subtypes in mice, resting NK cells predominantly express *Adrb2* (encoding β 2AR) at steady-state (Fig. 2 A). Interestingly, *Adrb2* expression in activated NK cells increased at day 2 PI (Fig. 2 A and Fig. S1 A), coinciding with NK cell infiltration into the white pulp (Fig. 1 B). Early activation of NK cells during viral infection has been previously shown to be mediated through activating receptors such as Ly49H, along with pro-inflammatory cytokines secreted by dendritic cells, including type I IFNs and IL-12 (Madera et al., 2016; Sun et al., 2012). To determine which signals contributed toward the up-regulation of *Adrb2* in NK cells during MCMV

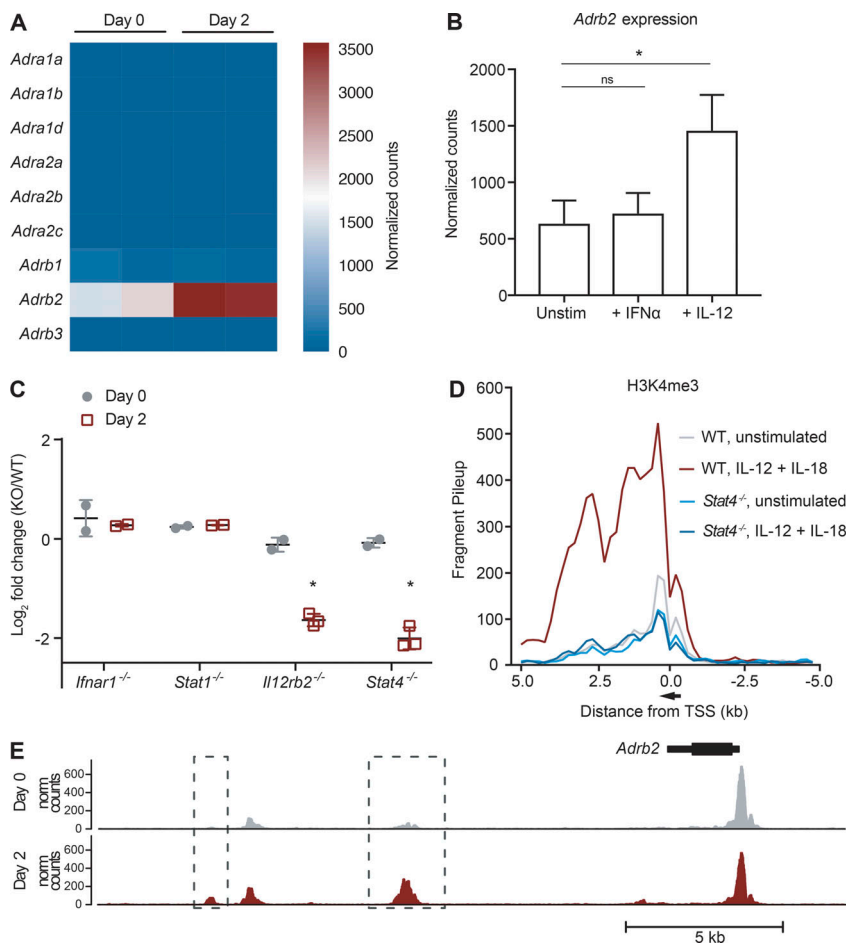


Figure 2. *Adrb2* is induced early after MCMV infection and dependent on IL-12 and STAT4 signaling. (A) Ly49H⁺ NK cells were sorted from the spleen of MCMV-infected WT mice, and RNA-seq was performed. Heatmap shows expression of the adrenergic receptor family of genes on splenic NK cells at day 0 or 2 PI (*n* = 2 samples per condition). (B) *Adrb2* expression on WT NK cells stimulated for 4 h with IL-12, IFN- α , or media alone, and measured by RNA-seq. Data are representative of two independent experiments with two or three samples per condition. (C) Mixed chimeras generated with bone marrow from WT mice (CD45.1) and *Il12r2*^{-/-}, *Stat4*^{-/-}, *Ifnar1*^{-/-}, or *Stat1*^{-/-} mice (CD45.2) were infected with MCMV, and splenic Ly49H⁺ NK cells were sorted at day 2 PI for RNA-seq. Differential expression of *Adrb2* is shown for various KO compared with WT NK cells (*n* = 2 to 3 samples per condition). (D) H3K4me3 ChIP was performed on WT or *Stat4*^{-/-} NK cells stimulated with IL-12 and IL-18, or media alone for 4 h, followed by Illumina NGS. H3K4me3 peaks are shown for the *Adrb2* locus, and normalized counts of fragments binned at 200 bp across a 10-kb window centered on the transcriptional start site (TSS). Data are representative of two independent experiments. (E) Representative tracks of the chromatin accessibility around the *Adrb2* locus on purified splenic Ly49H⁺ NK cells at steady-state and day 2 PI (top), as assessed by ATAC-seq. ATAC-seq peaks with a log₂ fold-change > 1 between both conditions are shown in boxes and quantified in graphs (bottom). Data are representative of three independent experiments with three or four replicates per condition. Statistical differences (*P* < 0.05) are indicated with a single star (*) and were determined using multiple hypothesis-corrected *P* values as calculated by DESeq2. Norm, normalized; Unstim, unstimulated. All bar plots show mean \pm SEM.

infection, we performed RNA-seq on purified NK cells stimulated ex vivo with either IFN- α or IL-12. *Adrb2* expression in NK cells increased after activation with IL-12, but not IFN- α (Fig. 2 B and Fig. S1 B), suggesting that IL-12 signaling is sufficient to induce the up-regulation of *Adrb2*. Interestingly, *Adrb2* expression increased further upon costimulation with IL-12 and IL-18, suggesting a synergistic effect of NF- κ B and STAT4 signaling (Fig. S1 C). To confirm whether *Adrb2* induction on NK cells was similarly regulated during MCMV infection, we generated mixed WT:KO bone marrow chimeric (mBMC) mice, and performed RNA sequencing (RNA-seq) on activated NK cells defective in type I IFN signaling (*Ifnar1*^{-/-} and *Stat1*^{-/-}) or IL-12 signaling (*Il12rb2*^{-/-} and *Stat4*^{-/-}). NK cells defective in either cytokine pathway expressed similar levels of *Adrb2* compared with WT NK cells at steady-state, suggesting that neither type I IFN nor IL-12 signaling impact *Adrb2* expression in the absence of infection (Fig. 2 C and Fig. S1 D). Similar to our findings in the ex vivo setting, following MCMV infection, NK cells deficient in the IL-12R or transcription factor STAT4 were impaired in their ability to up-regulate *Adrb2* at day 2 PI, whereas deficiency in the IFN alpha receptor (IFNAR) and STAT1 did not affect *Adrb2* expression (Fig. 2 C and Fig. S1 D).

Activation of NK cells by pro-inflammatory cytokines triggers dynamic epigenetic changes, allowing for the rapid

transcription of genes important in the effector response (Adams et al., 2018; Beaulieu et al., 2014; Lau et al., 2018; Rapp et al., 2017). Consistent with this notion, the abundance of the histone mark H3K4me3, which is generally associated with actively transcribed genes (Santos-Rosa et al., 2002), greatly increased around the *Adrb2* promoter region following treatment of NK cells with IL-12 ex vivo, a process that was dependent on STAT4 (Fig. 2 D). Moreover, the accessibility of several intergenic regions surrounding the *Adrb2* gene increased after infection, as revealed by an assay for transposase-accessible chromatin using sequencing (ATAC-seq; Fig. 2 E), suggesting these may be putative enhancer regions. Together, these experiments demonstrate that IL-12 signaling via STAT4 induces increased chromatin accessibility and transcriptional activation of *Adrb2* in activated NK cells.

Adrenergic signaling regulates optimal NK cell homeostasis, maturation, and effector function in a cell-intrinsic manner

Our observation that NK cells migrate toward adrenergic nerve fibers while up-regulating *Adrb2* during viral infection suggests that adrenergic signaling may be required for NK cell responses against MCMV. To address this possibility, we generated *Nkp46*^{Cre/+} *Adrb2*^{f/f} mice, in which *Adrb2* is specifically deleted in NK cells (referred to as NK-*Adrb2*^{-/-} mice hereafter). At

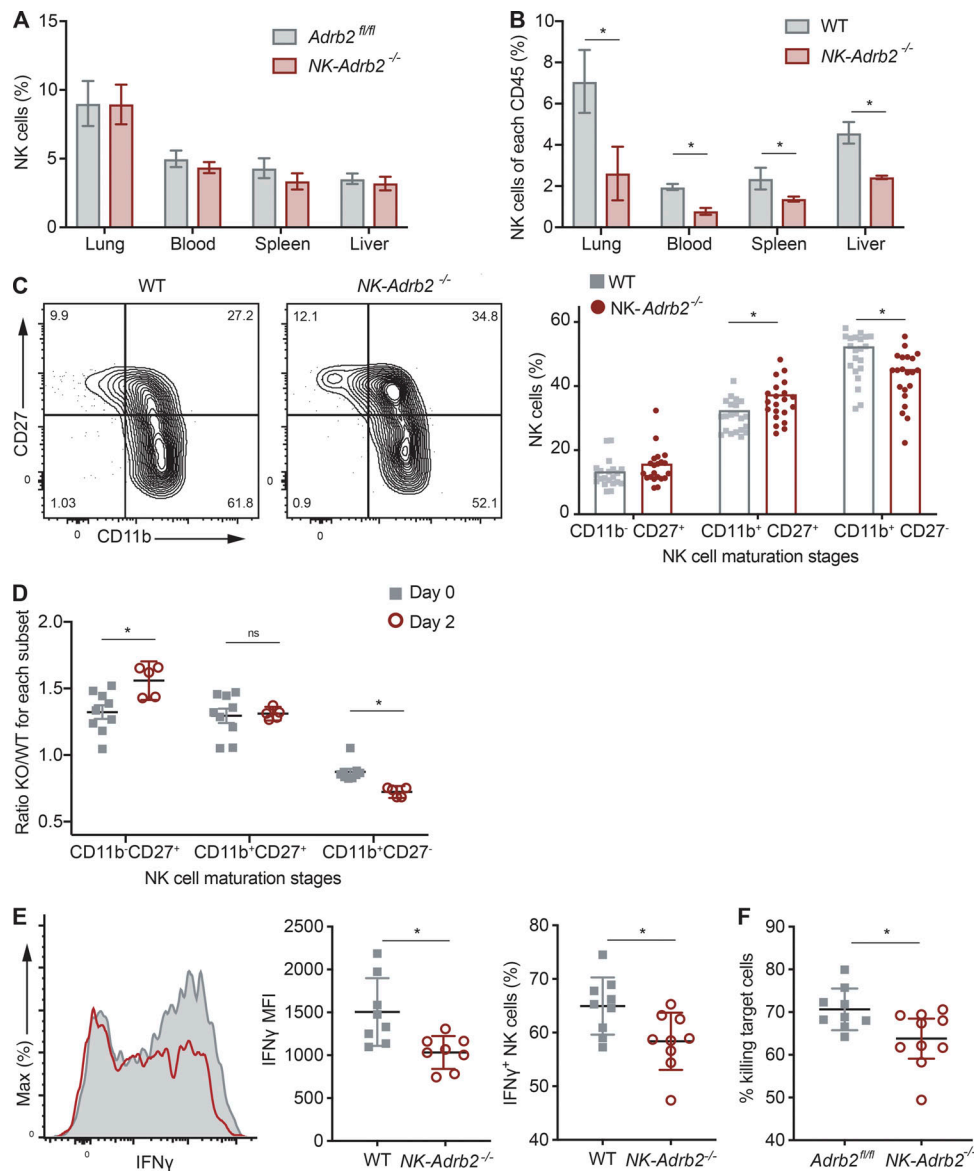


Figure 3. β 2AR promotes optimal NK cell homeostasis and function. (A and B) Quantification of NK cell percentages (NK1.1⁺ CD49b⁺ Lin⁻) between various organs as percentage of total CD45⁺ cells in *NK-Adrb2*^{-/-} or littermate *Adrb2*^{fl/fl} mice (A), or in mixed WT(CD45.1): *NK-Adrb2*^{-/-} (CD45.2) bone marrow chimeric (mBMC) mice (B) at steady-state. Representative of four different experiments with four to seven mice per group. (C) Representative flow plots showing the expression of maturation markers CD11b and CD27 in WT or *NK-Adrb2*^{-/-} NK cells from the peripheral blood of mBMC mice after bone marrow reconstitution. Graph shows the quantification of the percentage of NK cells expressing these markers. Data are pooled from three independent experiments with at least five mice per group. (D) The percentage of *NK-Adrb2*^{-/-} NK cells at each maturation stage (marked by CD27 and CD11b) was normalized to that of WT NK cells in mBMC mice, and quantified as a ratio at steady-state or day 2 PI. Data are pooled from two independent experiments with three or four mice per group. (E) Representative histogram (left) showing IFN- γ production in WT (gray, shaded) or *NK-Adrb2*^{-/-} NK cells (red), from mBMC mice infected with MCMV at day 2 PI. Graphs shows mean fluorescence intensity (MFI) of IFN- γ (middle) or percentage of IFN- γ producing cells (right) for WT or *NK-Adrb2*^{-/-} populations. Data are pooled from three independent experiments with three mice per group. (F) Percentage clearance of m157-expressing splenocytes (target cells) transferred into *NK-Adrb2*^{-/-} or littermate *Adrb2*^{fl/fl} mice 4 to 6 h after transfer, normalized to the number of *Ly49h*^{-/-} splenocytes (nontarget control cells) cotransferred. Data are representative of four independent experiments with four mice per group. For experiments in which two variables were compared across multiple conditions (A–D), statistical differences ($P < 0.05$) were calculated using Sidak’s multiple comparisons test (two-way ANOVA) and indicated with a single star (*). For experiments in which one variable was compared across two conditions (E and F), statistical differences ($P < 0.05$) were calculated using a two-tailed Student’s *t* test and indicated with a single star (*). All bar plots show mean \pm SEM.

steady-state, peripheral NK cell numbers, maturation, and receptor repertoire were comparable to those of littermate control mice (*NKp46*^{+/+} *Adrb2*^{fl/fl}), suggesting that adrenergic signaling is dispensable for NK cell development and homeostasis (Fig. 3 A and Fig. S1, E and F). These findings are consistent

with similar transgenic mice generated by Wieduwild et al. in this issue. However, in an mBMC setting, where *NK-Adrb2*^{-/-} NK cells develop in the same environment as WT NK cells, we observed a reduction in the frequency of *NK-Adrb2*^{-/-} NK cells across various organs (Fig. 3 B). To further confirm these findings, we

generated *Adrb2*-deficient NK cells using two alternative mouse models, *Vav1^{cre/+} Adrb2^{fl/fl}* mice and germline *Adrb2^{-/-}* mice. In a mBMC setting, deletion of *Adrb2* in NK cells using either genetic model resulted in a similar reduction in the frequency of circulating NK cells, while *Adrb2^{fl/fl}* (littermate WT) NK cells were found at a similar frequency compared with CD45.1 WT NK cells in mBMCs (Fig. S1 G).

We also observed modest differences in the acquisition of several maturation markers in the mBMC setting (Fig. 3 C). Interestingly, the maturation differences became even more pronounced when mBMC were challenged with MCMV (Fig. 3 D), suggesting that β 2AR may regulate the activation and terminal maturation of NK cells in a cell-intrinsic manner during viral infection.

We next investigated whether direct adrenergic signaling was required for NK cell effector function. During MCMV infection, NK cell activation results in the rapid production and release of IFN- γ and cytotoxic granules containing perforin and granzymes. *NK-Adrb2^{-/-}* and littermate NK cells degranulated similarly during ex vivo stimulation with pro-inflammatory cytokines, or PMA and ionomycin (Fig. S1, H and I), consistent with findings from Wieduwild et al. (2020). In the mBMC infected with MCMV, *NK-Adrb2^{-/-}* NK cells exhibited a modest albeit reproducible defect in IFN- γ production, which was independent of their maturation stage (Fig. 3 E and (Fig. S1 J)). To test whether such defect could have a functional relevance for NK cell-mediated killing, we transferred m157-expressing target splenocytes and nontarget controls into either *NK-Adrb2^{-/-}* or littermate mice, and assessed their ability to clear target cells in vivo. Compared with WT mice, *NK-Adrb2^{-/-}* mice cleared target cells less efficiently (Fig. 3 F), suggesting that adrenergic signals present during a viral infection, but absent in an ex vivo setting, may be able to control certain effector functions of NK cells.

Adrenergic signaling drives optimal adaptive NK cell responses and protection during viral challenge

During MCMV infection, Ly49H⁺ NK cells can expand 100–1,000-fold to increase the pool of effector cells, an “adaptive” feature required for the proper control of the virus (Beaulieu et al., 2014; Sun et al., 2009). Given its modest role in modulating early NK cell effector functions, we investigated whether adrenergic signaling is required for adaptive NK cell responses. To directly test this, we adoptively transferred equal numbers of congenically distinct *NK-Adrb2^{-/-}* and WT NK cells into *Klra8^{-/-}* (Ly49H-deficient) mice, infected these recipients with MCMV, and measured the expansion of transferred Ly49H⁺ NK cells in peripheral blood at various time points (Fig. 4 A). Whereas WT Ly49H⁺ NK cells underwent robust expansion, *NK-Adrb2^{-/-}* Ly49H⁺ NK cells exhibited impaired expansion, representing less than half of all transferred effector cells at day 7 PI (Fig. S2 A and Fig. 4 B). NK cells from littermate controls expanded comparable to WT controls in this setting, while *Adrb2*-deficient NK cells generated using two alternative genetic models exhibited a similar expansion defect (Fig. S2, B and C). Diminished numbers of *NK-Adrb2^{-/-}* NK cells were also observed at memory time points (Fig. S2 A), likely a consequence of defects observed in early expansion, as overall WT:KO ratios remained stable past day 7 PI, during the contraction and memory phases (Fig. S2 D).

Adrenergic signaling has been involved in the rapid redistribution of lymphocytes between lymphoid and nonlymphoid organs (Løeper, 1904; Pedersen et al., 2016), raising the possibility that the observed expansion defect of *NK-Adrb2^{-/-}* NK cells in peripheral blood could be due to impaired circulation or trafficking. However, following adoptive transfer and MCMV infection, we observed a consistent reduction in *NK-Adrb2^{-/-}* NK cell frequencies in both lymphoid and nonlymphoid organs (Fig. 4 C), suggesting that adrenergic signaling is required for general NK cell expansion and not restricted to any particular organ.

We next investigated whether direct signaling by adrenergic fibers was required for robust NK cell expansion. We antagonized the activity of adrenergic fibers with oxidopamine (6-OHDA) and metyrosine (MTR), as described previously (Murray et al., 2017; Staedtke et al., 2018). WT NK cells transferred into vehicle-treated *Ly49h^{-/-}* recipient mice expanded significantly more at day 7 PI than *Adrb2*-deficient NK cells, as reported in Fig. 4 C, and also significantly more than WT NK cells transferred into antagonist-treated *Ly49h^{-/-}* mice, suggesting that adrenergic signaling is required for the optimal expansion of WT NK cells (Fig. 4 D). Furthermore, the expansion of *Adrb2*-deficient NK cells transferred into either vehicle- or antagonist-treated mice was comparable to that of WT NK cells in the antagonist-treated mice, suggesting that the impaired NK cell expansion observed in antagonist-treated mice occurs in an *Adrb2*-dependent manner (Fig. 4 D).

We next sought to determine how β 2AR deficiency limited NK cell expansion during MCMV infection, and whether this would result in decreased host protection. We adoptively transferred NK cells labeled with the division-tracking dye CellTrace Violet (CTV), and found that *NK-Adrb2^{-/-}* NK cells did not divide as efficiently as their WT counterparts (Fig. 5, A and B). *NK-Adrb2^{-/-}* NK cells did not have elevated levels of apoptosis as measured by FLICA staining (Fig. S2 E), suggesting that a proliferation defect underlies the diminished clonal expansion observed.

To confirm that the diminished proliferative capacity of *NK-Adrb2^{-/-}* NK cells is critical for protection against MCMV infection, we transferred purified NK cells from either *NK-Adrb2^{-/-}* mice or littermate controls into *Rag2^{-/-} Il2rg^{-/-}* mice (which lack T, B, and NK cells), and measured their survival and viral load after MCMV challenge (Fig. 5, C and D). Mice receiving *NK-Adrb2^{-/-}* NK cells were significantly more susceptible to MCMV than those receiving WT NK cells (Fig. 5 C). Furthermore, although mice receiving *Adrb2*-deficient NK cells had a comparable viral load to those receiving WT NK cells at earlier infection time points, they bore a much higher viral load at later infection time points, coinciding with the peak of NK cell expansion in this model (Fig. 5 D and Fig. S2 F). Consequently, transfer of WT NK cells, but not *NK-Adrb2^{-/-}* NK cells, increased the median survival of infected *Rag2^{-/-} Il2rg^{-/-}* mice compared with mice that received no cells. Thus, our findings suggest that cell-intrinsic adrenergic signaling is required for optimal adaptive NK cell responses and host protection against viral infection (Fig. 5 E).

A growing body of evidence supports the notion that the adaptive features of NK cell responses, including prolific expansion and memory formation, are critical for host protection against viral infection (Lau and Sun, 2018; O’Sullivan et al., 2015;

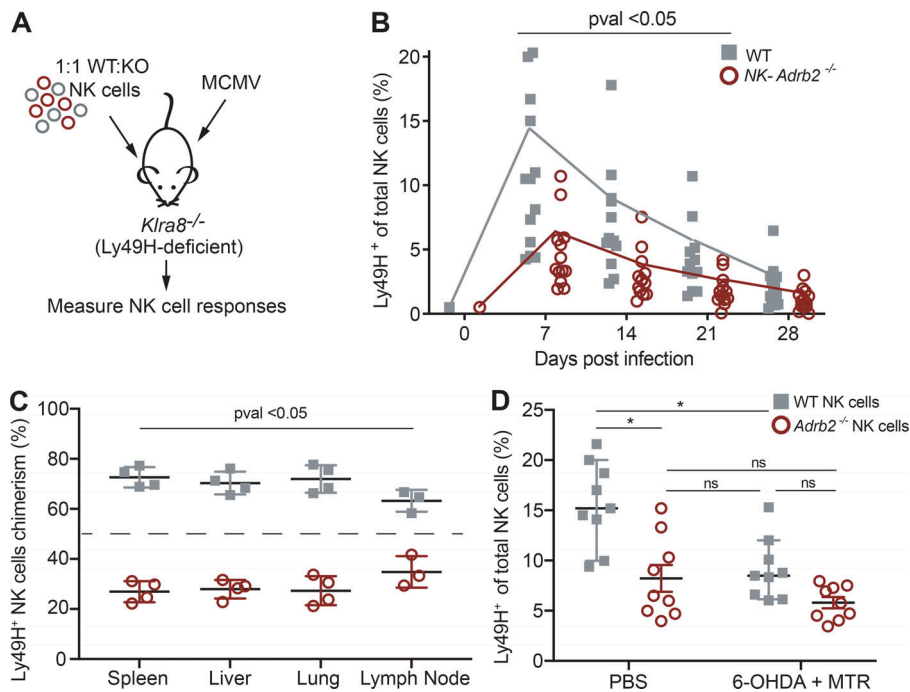


Figure 4. *Adb2* is required for robust NK cell expansion. (A) Experimental design. Equal numbers of Ly49H⁺ splenic NK cells from WT (CD45.1) and *NK-Adrb2*^{-/-} mice (CD45.2) were transferred into Ly49H-deficient mice (CD45.1 × CD45.2) and challenged with MCMV. (B) The percentage of WT and *NK-Adrb2*^{-/-} Ly49H⁺ NK cells was quantified in peripheral blood weekly as indicated. Data are pooled from four independent experiments with at least five mice per group. (C) The ratio of transferred WT and *NK-Adrb2*^{-/-} Ly49H⁺ NK cells was quantified in various peripheral organs at day 35 PI. Data are representative of two independent experiments with five mice per group. (D) *Ly49h*^{-/-} recipient mice were treated with adrenergic antagonists (6-OHDA and MTR) or with vehicle control, and the percentage of transferred WT and *Adrb2*-deficient NK cells in peripheral blood was quantified at day 7 PI. Data are pooled from two independent experiments with four to five mice per group. Statistical differences (P < 0.05) were calculated using Sidak's multiple comparisons test (two-way ANOVA) and indicated with a single star (*). All bar plots show mean ± SEM.

Sun et al., 2009). Here, we reveal that costimulatory signals provided through β2ARs regulate these processes and are required for NK cell-mediated protection against MCMV. Global, transient stimulation of glucocorticoid and adrenergic pathways, as occurs during the fight-or-flight response or stroke episodes, have previously been described to modulate NK cell recruitment and function (Breen et al., 2016; Izumo et al., 2013; Prass et al., 2003; Quatrini et al., 2017, 2018b). However, whether NK cells can directly sense adrenergic signals had not been previously determined. Consistent with findings from Wieduwild et al. (2020), cell-intrinsic adrenergic signaling was largely dispensable for NK cell development, homeostasis, and early effector function against MCMV. In contrast to the early innate responses, in the present study we show that cell-intrinsic adrenergic signaling was necessary to elicit robust adaptive NK cell responses, revealed in adoptive transfer experiments where NK cells could undergo large proliferative bursts. Mainly, the proliferative capacity of NK cells was essential to control viral replication in immune-deficient hosts and improve survival against MCMV.

Interestingly, Wieduwild et al. (2020) show that indirect, cell-extrinsic adrenergic signaling acting through a non-neuronal, nonhematopoietic compartment negatively regulates IFN-γ production by liver NK cells, reducing host immune defense against viral challenge. In this case, the improved survival of *Adrb2*^{-/-} mice was attributed to increased IFN-γ production, a hallmark of the early NK cell effector function. Thus, we believe that adrenergic signals control the function and proliferation of NK cells through distinct, nonexclusive mechanisms that differ in the timing and nature of the interactions between the immune and ANS. These complementary layers of regulation should be considered when designing therapies to target both NK cell activity and adrenergic pathways, or when given in combination with β-blockers commonly used in the clinic.

Recent reports have suggested that neural mediators (e.g., neuropeptides and catecholamines) can modulate group 2 innate lymphoid cell (ILC2) responses in the gut and lung (Cardoso et al., 2017; Klose et al., 2017; Moriyama et al., 2018; Wallrapp et al., 2017). Although they share a common lymphoid progenitor, conventional NK cells and ILC2s have distinct developmental requirements and functions. Whereas ILC2s are tissue-resident and exert their immune-modulatory properties through cytokine signals to mediate type II inflammation, NK cells are circulating and respond against MCMV infection via antigen receptor engagement (along with pro-inflammatory cytokines) to drive a potent type I immune response. Thus, we believe that signals traditionally associated with the ANS differentially regulate tissue-resident versus circulating lymphocytes during inflammatory or infectious states. Although NK cells are found in proximity to adrenergic neurons shortly after infection, and ablation of adrenergic neurons impairs NK cell proliferation in an *Adrb2*-dependent manner, the precise nature and duration of the interaction require further investigation. Future studies will also test whether the response of other circulating lymphocytes, such as virus-specific CD8⁺ T cells, may be controlled by adrenergic signaling in a similar fashion to Ly49H⁺ NK cells. In summary, our findings suggest that cell-intrinsic adrenergic signaling promotes adaptive NK cell responses during viral infection and provide new insights into how the nervous system may coordinate the immune response against pathogens.

Materials and methods

Mice

Mice used in this study were housed and bred at Memorial Sloan Kettering Cancer Center (MSKCC) under specific pathogen-free conditions. Experiments were conducted using age- and gender-matched mice (typically 6–10 wk old) in accordance with

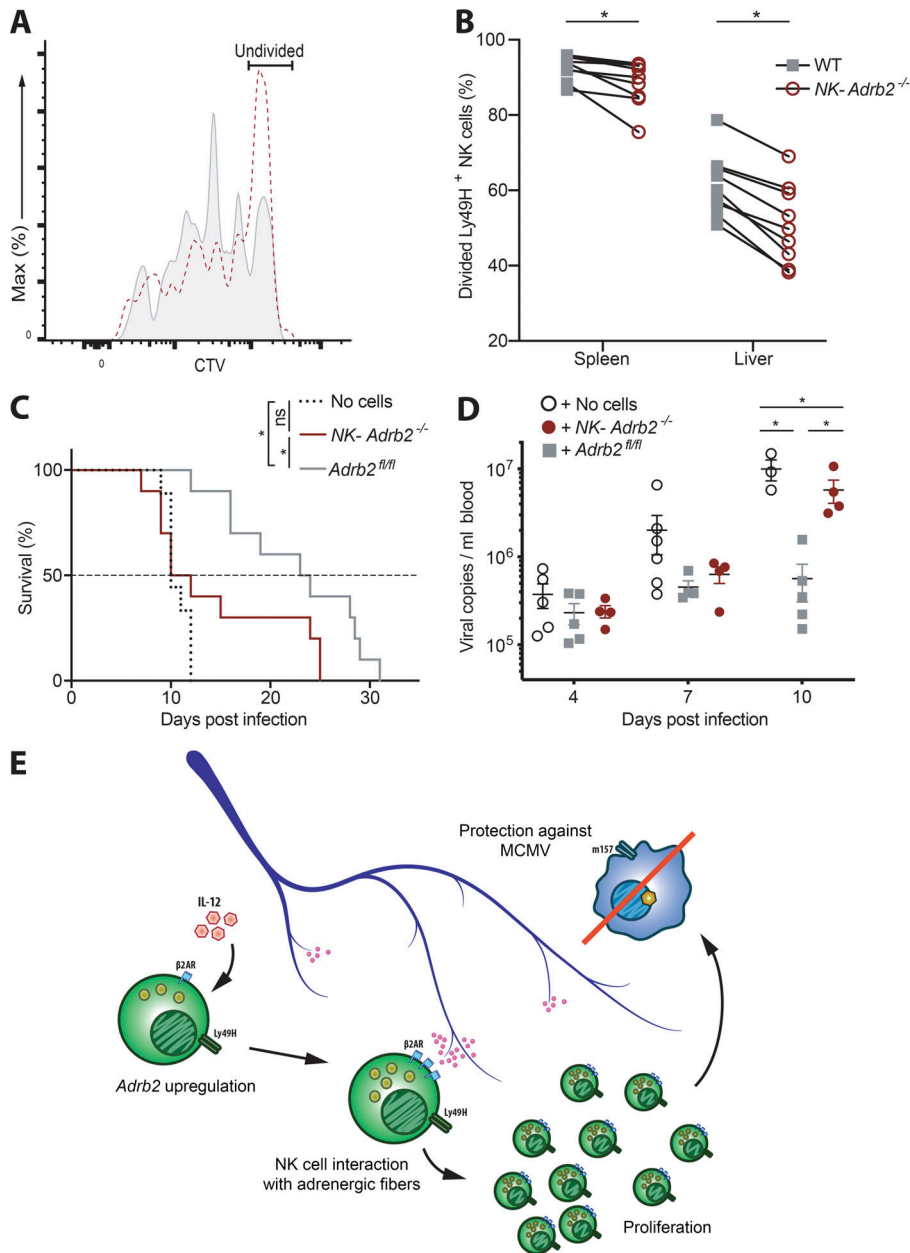


Figure 5. Cell-intrinsic adrenergic signaling drives NK cell proliferation and protection against MCMV. (A and B) As in Fig. 4 B, except splenocytes were labeled with CTV before transfer. **(A)** Representative histogram of Ly49H⁺ NK cells recovered from spleen at day 3.5 PI. **(B)** Quantification of the percentages of Ly49H⁺ NK cells that have undergone at least one division. Data are representative of three independent experiments with four or five mice per group. Statistical differences ($P < 0.05$) were calculated using Sidak's multiple comparisons test (two-way ANOVA) and indicated with a single star (*). **(C)** 10^5 splenic Ly49H⁺ NK cells from *NK-Adrb2*^{-/-} or littermate *Adrb2*^{fl/fl} mice were transferred into *Rag2*^{-/-} *Il2rg*^{-/-} mice. Some mice received no cells as control. All mice were challenged with MCMV, and survival was calculated using the Kaplan-Meier estimator. Data are pooled from two independent experiments with five mice per group. Statistical differences ($P < 0.05$) were determined using Mantel-Cox test and indicated with a single star (*). **(D)** As in C, except peripheral blood from recipient mice was drawn at indicated time points and used to quantify viral titers. Data are representative of two independent experiments with four to six mice per group. Statistical differences ($P < 0.05$) were calculated using Tukey's multiple comparisons test (two-way ANOVA) and indicated with a single star (*). **(E)** Model: Pro-inflammatory cytokines produced during viral infection induce the up-regulation of β 2AR on NK cells. Concomitantly, NK cells migrate in closer proximity to splenic adrenergic neurons, which allows them to receive adrenergic signals through β 2AR. This results in optimal NK cell expansion and proliferation, which is in turn required for the control of viral infection and protection against MCMV. All bar plots show mean \pm SEM.

approved institutional protocols from the Institutional Animal Care and Use Committee at MSKCC. The strains used in this study, all on the C57BL/6 background, are listed below: C57BL/6 (CD45.2), B6.SJL (CD45.1), *Adrb2*^{fl/fl} (Hinoi et al., 2008), *Klra8*^{-/-} (Ly49H-deficient; Fodil-Cornu et al., 2008), *Ncr1*^{9fp} (Gazit et al., 2006), *Nkp46iCre* (referred to as *NKp46*^{Cre}; Narni-Mancinelli et al., 2011), *Vav1-iCre* (referred to as *Vav1*^{Cre}; The Jackson Laboratory), *Adrb2*^{-/-} (Chruscinski et al., 1999), *Rag2*^{-/-} *Il2rg*^{-/-} (Taconic), *Rosa26*^{tdTom} (The Jackson Laboratory), *Stat1*^{-/-} (Meraz et al., 1996), and *Stat4*^{-/-} (Kaplan et al., 1996). B6 CD45.1 \times CD45.2, *Klra8*^{-/-} CD45.1 \times CD45.2, *NKp46*^{Cre} \times *Rosa26*^{tdTom}, and *NKp46*^{Cre} \times *Adrb2*^{fl/fl} mice were generated at MSKCC. *Adrb2*^{fl/fl} mice were generously provided by Dr. Daniel Mucida (The Rockefeller University, New York, NY) with the permission of Dr. Gerard Karsenty (Columbia University, New York, NY). Adoptive transfer studies and the generation of mixed bone

marrow chimeric mice were performed as previously described (Beaulieu et al., 2014; Sun et al., 2009).

Virus infection

MCMV (Smith strain) viral stocks were prepared by serial passage through BALB/c hosts (twice), and later dissociation of salivary glands 3 wk PI. For adoptive transfer studies, animals were infected i.p. with 7.5×10^2 PFU of MCMV. For mBMC infections, mice received 7.5×10^3 PFU of MCMV. For survival studies in *Rag2*^{-/-} *Il2rg*^{-/-} recipients, mice were infected by i.p. injection of 10^4 PFU of MCMV.

Histology

For immunofluorescence staining, spleens from *NKp46*-tdTomato or *NK1.1*-GFP reporter mice were incubated overnight at room temperature with fixative solution (1% paraformaldehyde,

80 mM L-lysine, and 10 μ M sodium periodate in phosphate buffer), washed with PBS, and dehydrated in 30% sucrose (in PBS) overnight. Spleens were placed in TissueTek optimal cutting temperature compound (Sakura) and frozen in dry ice and ethanol. 20- μ m spleen cryosections were rehydrated in PBS, blocked with 5% goat serum and 2% FCS in PBS, and stained with rabbit anti-TH (AB152, Millipore) in antibody diluent (2% FCS in PBS) overnight at 4°C. Slides were washed twice with antibody diluent and stained with Alexa 647 goat anti-rabbit IgG (A21244, Invitrogen), and Alexa 488 rabbit anti-GFP (A21311, Invitrogen) when necessary. Slides were stained with DAPI nuclear staining and preserved with Pro-Long glass mountant (Thermo Fisher). Images were acquired using a Zeiss LSM 880 confocal microscope (Zeiss) and processed as TIFF files using ImageJ software (open source). For quantification of NK cell–neuron distances, single-channel images were converted into a binary format, and black pixels were quantified using the “analyze particle” function. The resulting regions of interest were measured with the “measure” function to obtain the xy-positions of the regions of interest. The cell contours and the xy-positions were exported, and the distances between neurons and NK cells were measured with the R software.

Flow cytometry and cell sorting

Cell surface staining of single-cell suspensions from various organs was performed using fluorophore-conjugated antibodies (BD Biosciences, eBioscience, BioLegend, Tonbo, R&D Systems). Intracellular staining was performed by fixing and permeabilizing with the BD Cytofix/Cytoperm Fixation/Permeabilization Solution kit for staining cytosolic proteins and cytokines.

Flow cytometry and cell sorting were performed on the LSR II and Aria II cytometers (BD Biosciences), respectively. For RNA-seq experiments, quantitative real-time PCR (RT-qPCR), and NK cell transfers into *Rag2*^{-/-} *Il2rg*^{-/-}, cell populations were sorted to >95% purity. Data were analyzed with FlowJo9 software (Tree Star). Flow cytometry of purified lymphocytes was performed using the following fluorophore-conjugated antibodies: CD3 ϵ (17A2), TCR β (H57-597), CD19 (ID3), F4/80 (BM8.1), Ly6G (1A8), NK1.1 (PK136), NKp46 (29A1.4), Ly49H (3D10), CD45.1 (A20), CD45.2 (104), CD11b (M1/70), CD27 (LG.3A10), KLRG1 (2F1), Ly49D (4E5), Ly49A (YE1/48.10.6), Ly49C/I (5E6), CX3CR1 (SA011F11), CD25 (PC61), CD69 (H1.2F3), Granzyme B (GB11), IFN- γ (XMG1.2), CD107a (1D4B), and CD49b (DX5). NK cell proliferation was analyzed by labeling cells with 5 μ M CTV (Invitrogen) before transfer, and CTV labeling was performed according to manufacturer protocol. NK cell apoptosis was measured by staining transferred cells with FAM-DEVD-FMK FLICA reagent (FLICA, ImmunoChemistry Technologies) to measure active caspase-3/7 in live cells according to the manufacturer protocol.

Assessment of in vivo NK cell clearance of target cells

To study the killing of target cells by Ly49H⁺ NK cells in vivo, equal numbers of m157-expressing splenocytes (targets) and Ly49H-deficient splenocytes (controls) were transferred into

either *NK-Adrb2*^{-/-} or littermate mice. Blood was collected 4–6 h following transfer, and the percentage of target killing was calculated as the ratio of remaining targets to control cells, normalized to the initial ratio before transfer.

Ablation and antagonization of adrenergic neurons

Chemical ablation of adrenergic nerves was performed by treating *Ly49h*^{-/-} recipient mice with two doses of 6-OHDA (250 mg/kg, Sigma) and MTR (80 mg/kg, Santa Cruz Biotech, sc-219470) at day -1 and day 3 PI. Equal numbers of *Vav1*^{cre+} *Adrb2*^{fl/fl} and congenically distinct WT Ly49H⁺ NK cells were transferred intravenously, and numbers and frequency of transferred cells analyzed at day 7 PI.

RNA-seq, H3K4Me3 chromatin immunoprecipitation (ChIP),

DNA sequencing, and analysis

Isolation of RNA, library preparation, and data analysis of ex vivo NK cells PI and in vitro stimulated NK cells have been previously described (Geary et al., 2018; Lau et al., 2018; Rapp et al., 2017). Briefly, 1.5–10 \times 10⁴ Ly49H⁺ NK cells (TCR β ⁻ CD19⁻ CD3 ϵ ⁻ NK1.1⁺ CD49b⁺ Ly49H⁺) were sorted from C57BL/6 mice, or WT:KO (*Stat4*^{-/-}, *Ifnar1*^{-/-}, *Stat1*^{-/-}) mBMC mice at days 0 and 2 after MCMV infection. For in vitro stimulations, 5–8 \times 10⁴ NK cells were sorted for purity and incubated overnight with 20 ng/ml of IL-12, or 100 U/ml of IFN α . RNA was extracted by Trizol and prepared for library construction and Illumina Next generation sequencing.

Isolation of DNA for H3k4me3 ChIP-seq and data analysis was performed and analyzed as described previously (Rapp et al., 2017). Briefly, 5–10 \times 10⁶ NK cells (TCR β ⁻ CD19⁻ CD3 ϵ ⁻ NK1.1⁺ CD49b⁺) from WT or *Stat4*-deficient mice were sorted from pooled spleens and incubated overnight (~18 h) with IL-12 (20 ng/ml) and IL-18 (10 ng/ml). DNA and proteins were cross-linked for 8 min using 1% formaldehyde. ChIP was performed using 1 mg of rabbit polyclonal anti-trimethyl Histone H3 (Lys4) antibody (H3K4me3, Millipore, 07473), and prepared for Illumina next-generation sequencing.

RT-qPCR

5 \times 10⁴ purified (>95% purity) NK cells were stimulated with IL-12 (20 ng/ml), IL-18 (10 ng/ml), or a combination of both, or were left untreated for 3 h, and RNA was extracted with the PicoPure RNA Isolation Kit (Arcturus). cDNA was synthesized using the QuantiTect Reverse transcription kit (Qiagen). RT-qPCR with cDNA as a template was performed in triplicate on an ABI QuantStudio 6 Flex RT-qPCR machine, using Taqman Probes for *Adrb2* (Mm02524224_s1, Thermo Fisher) and *Actb* (Mm02619580_g1, Thermo Fisher). Relative *Adrb2* gene expression was normalized to that of *Actb* using the 2^{- Δ Ct} method.

Quantification of viral titers from peripheral blood

At indicated time points, 200 μ l of peripheral blood was drawn retro-orbitally, and total DNA was extracted using the QIAamp DNA Blood Mini Kit (QIAGEN). Viral copy number in eluted DNA was determined in triplicate by quantitative PCR using iQ SYBR mastermix (Bio-Rad) using the MCMV-specific primers IE-1 (forward: 5'-TCGCCATCGTTTCGAGA-3', reverse: 5'-TCT

CGTAGGTCCACTGACGGA-3'). A standard curve of MCMV plasmid DNA was used to calculate the viral copy number in sample DNA by correlating their quantitation cycle (Cq) values.

Data availability

The sequencing data supporting these findings (RNA-seq, ATAC-seq, and ChIP-seq) have been deposited in the Gene Expression Omnibus public database under accession no. GSE106139. All other data presented in the current study are available from the corresponding author upon reasonable request.

Statistical analyses

Unless otherwise indicated, data represented as bar graphs are plotted as mean \pm SEM. For experiments in which one variable was compared across two conditions, statistical differences were calculated using a two-tailed Student's *t* test. For experiments in which one variable was compared in more than two conditions, statistical differences were calculated using a Tukey's multiple comparison test (one-way ANOVA). For experiments in which two variables were compared across multiple conditions, statistical differences were calculated using Sidak's or Tukey's multiple comparisons test (two-way ANOVA). Statistical differences in survival curves were determined by Mantel-Cox test analysis. A *P* value of <0.05 was used as the significance cutoff and is indicated with a single star (*). Statistical analysis was performed using GraphPad Prism software.

Online supplemental material

Fig. S1 shows the expression of *Adrb2* in NK cells under IL-12 stimulation and infection as assayed with RT-qPCR; the maturation state and ex vivo stimulation of *NK-Adrb2*^{-/-} NK cells compared with littermate controls; and the mBMC reconstitution of *Adrb2*^{-/-} NK cells (obtained with different genetic models) and IFN- γ production upon infection compared with WT controls. **Fig. S2** shows the expansion of *Adrb2*^{-/-} NK cells (obtained with different genetic models) and littermate controls compared with congenically distinct WT cells throughout infection; the percentage of KO and WT NK cells undergoing apoptosis during infection; and the change in viral titers during infection.

Acknowledgments

We thank members of the Sun laboratory for technical support, experimental assistance, insightful comments, and helpful discussions. S. Sheppard and H. Kim provided critical experimental assistance. D. Artis and A. Schietinger provided critical feedback, and D. Artis (Weill Cornell Medicine, New York, NY), E. Vivier (Aix-Marseille University, Marseille, France), S. Vidal (McGill University, Montreal, Canada), D. Mucida (The Rockefeller University, New York, NY), and G. Karsenty (Columbia University, New York, NY) provided mice critical to these studies. We thank S. Ugolini and E. Wieduwild for sharing their unpublished data and manuscript.

C. Diaz-Salazar was supported by a Fulbright student grant awarded by the Commission for Cultural, Educational and Scientific Exchange between the United States and Spain. R. Bou-

Puerto was supported by a "la Caixa" Fellowship from "la Caixa" Foundation (LCF/BQ/AA17/11610016). A.M. Mujal was supported by a T32 award from the National Institutes of Health (CA009149), and an Irvington Postdoctoral Fellowship from the Cancer Research Institute. C.M. Lau is a Cancer Research Institute-Carson Family Fellow. J.C. Sun was supported by the Ludwig Center for Cancer Immunotherapy, the American Cancer Society, the Burroughs Wellcome Fund, and the National Institutes of Health (AI100874, AI130043, and P30CA008748).

Author contributions: C. Diaz-Salazar, R. Bou-Puerto, and A.M. Mujal performed experiments. C. Diaz-Salazar, R. Bou-Puerto, A.M. Mujal, C.M. Lau, M. von Hoesslin, D. Zehn, and J.C. Sun analyzed the data. C. Diaz-Salazar and J.C. Sun designed the study and wrote the manuscript.

Disclosures: The authors declare no competing interests exist.

Submitted: 26 March 2019

Revised: 23 October 2019

Accepted: 13 January 2020

References

- Adams, N.M., C.M. Lau, X. Fan, M. Rapp, C.D. Geary, O.E. Weizman, C. Diaz-Salazar, and J.C. Sun. 2018. Transcription Factor IRF8 Orchestrates the Adaptive Natural Killer Cell Response. *Immunity*. 48:1172-1182.e6. <https://doi.org/10.1016/j.immuni.2018.04.018>
- Andrews, D.M., H.E. Farrell, E.H. Densley, A.A. Scalzo, G.R. Shellam, and M.A. Degli-Esposti. 2001. NK1.1+ cells and murine cytomegalovirus infection: what happens in situ? *J. Immunol.* 166:1796-1802. <https://doi.org/10.4049/jimmunol.166.3.1796>
- Arase, H., E.S. Mocarski, A.E. Campbell, A.B. Hill, and L.L. Lanier. 2002. Direct recognition of cytomegalovirus by activating and inhibitory NK cell receptors. *Science*. 296:1323-1326. <https://doi.org/10.1126/science.1070884>
- Beaulieu, A.M., C.L. Zawislak, T. Nakayama, and J.C. Sun. 2014. The transcription factor Zbtb32 controls the proliferative burst of virus-specific natural killer cells responding to infection. *Nat. Immunol.* 15:546-553. <https://doi.org/10.1038/ni.2876>
- Bekiaris, V., O. Timoshenko, T.Z. Hou, K. Toellner, S. Shakib, F. Gaspal, F.M. McConnell, S.M. Parnell, D. Withers, C.D. Buckley, et al. 2008. Ly49H+ NK cells migrate to and protect splenic white pulp stroma from murine cytomegalovirus infection. *J. Immunol.* 180:6768-6776. <https://doi.org/10.4049/jimmunol.180.10.6768>
- Bigler, M.B., S.B. Egli, C.M. Hysek, G. Hoenger, L. Schmied, F.S. Baldin, F.A. Marquardsen, M. Recher, M.E. Liechti, C. Hess, and C.T. Berger. 2015. Stress-Induced In Vivo Recruitment of Human Cytotoxic Natural Killer Cells Favors Subsets with Distinct Receptor Profiles and Associates with Increased Epinephrine Levels. *PLoS One*. 10:e0145635. <https://doi.org/10.1371/journal.pone.0145635>
- Breen, M.S., N. Beliakova-Bethell, L.R. Mujica-Parodi, J.M. Carlson, W.Y. Ensign, C.H. Woelk, and B.K. Rana. 2016. Acute psychological stress induces short-term variable immune response. *Brain Behav. Immun.* 53:172-182. <https://doi.org/10.1016/j.bbi.2015.10.008>
- Cardoso, V., J. Chesné, H. Ribeiro, B. Garcia-Cassani, T. Carvalho, T. Bouchery, K. Shah, N.L. Barbosa-Morais, N. Harris, and H. Veiga-Fernandes. 2017. Neuronal regulation of type 2 innate lymphoid cells via neuro-medin U. *Nature*. 549:277-281. <https://doi.org/10.1038/nature23469>
- Chruscinski, A.J., D.K. Rohrer, E. Schauble, K.H. Desai, D. Bernstein, and B.K. Kobilka. 1999. Targeted disruption of the beta2 adrenergic receptor gene. *J. Biol. Chem.* 274:16694-16700. <https://doi.org/10.1074/jbc.274.24.16694>
- Daniels, K.A., G. Devora, W.C. Lai, C.L. O'Donnell, M. Bennett, and R.M. Welsh. 2001. Murine cytomegalovirus is regulated by a discrete subset of natural killer cells reactive with monoclonal antibody to Ly49H. *J. Exp. Med.* 194:29-44. <https://doi.org/10.1084/jem.194.1.29>
- Dokun, A.O., S. Kim, H.R. Smith, H.S. Kang, D.T. Chu, and W.M. Yokoyama. 2001. Specific and nonspecific NK cell activation during virus infection. *Nat. Immunol.* 2:951-956. <https://doi.org/10.1038/ni714>

- Fodil-Cornu, N., S.H. Lee, S. Belanger, A.P. Makrigrannis, C.A. Biron, R.M. Buller, and S.M. Vidal. 2008. Ly49h-deficient C57BL/6 mice: a new mouse cytomegalovirus-susceptible model remains resistant to unrelated pathogens controlled by the NK gene complex. *J. Immunol.* 181: 6394–6405. <https://doi.org/10.4049/jimmunol.181.9.6394>
- Gabanyi, I., P.A. Muller, L. Feighery, T.Y. Oliveira, F.A. Costa-Pinto, and D. Mucida. 2016. Neuro-immune Interactions Drive Tissue Programming in Intestinal Macrophages. *Cell.* 164:378–391. <https://doi.org/10.1016/j.cell.2015.12.023>
- Gazit, R., R. Gruda, M. Elboim, T.I. Arnon, G. Katz, H. Achdout, J. Hanna, U. Qimron, G. Landau, E. Greenbaum, et al. 2006. Lethal influenza infection in the absence of the natural killer cell receptor gene Ncr1. *Nat. Immunol.* 7:517–523. <https://doi.org/10.1038/ni1322>
- Geary, C.D., and J.C. Sun. 2017. Memory responses of natural killer cells. *Semin. Immunol.* 31:11–19. <https://doi.org/10.1016/j.smim.2017.08.012>
- Geary, C.D., C. Krishna, C.M. Lau, N.M. Adams, S.V. Gearty, Y. Pritykin, A.R. Thomsen, C.S. Leslie, and J.C. Sun. 2018. Non-redundant ISGF3 Components Promote NK Cell Survival in an Auto-regulatory Manner during Viral Infection. *Cell Reports.* 24:1949–1957.e6. <https://doi.org/10.1016/j.celrep.2018.07.060>
- Godinho-Silva, C., F. Cardoso, and H. Veiga-Fernandes. 2019. Neuro-Immune Cell Units: A New Paradigm in Physiology. *Annu. Rev. Immunol.* 37: 19–46. <https://doi.org/10.1146/annurev-immunol-042718-041812>
- Grégoire, C., C. Cognet, L. Chasson, C.A. Coupet, M. Dalod, A. Reboldi, J. Marvel, F. Sallusto, E. Vivier, and T. Walzer. 2008. Intrasplenic trafficking of natural killer cells is redirected by chemokines upon inflammation. *Eur. J. Immunol.* 38:2076–2084. <https://doi.org/10.1002/eji.200838550>
- Gumá, M., A. Angulo, C. Vilches, N. Gómez-Lozano, N. Malats, and M. López-Botet. 2004. Imprint of human cytomegalovirus infection on the NK cell receptor repertoire. *Blood.* 104:3664–3671. <https://doi.org/10.1182/blood-2004-05-2058>
- Hinoi, E., N. Gao, D.Y. Jung, V. Yadav, T. Yoshizawa, M.G. Myers Jr., S.C. Chua Jr., J.K. Kim, K.H. Kaestner, and G. Karsenty. 2008. The sympathetic tone mediates leptin's inhibition of insulin secretion by modulating osteocalcin bioactivity. *J. Cell Biol.* 183:1235–1242. <https://doi.org/10.1083/jcb.200809113>
- Izumo, T., T. Maekawa, Y. Horii, Y. Fujisaki, M. Ida, Y. Furukawa, Y. Ono, Y. Kiso, Y. Kitagawa, H. Shibata, and K. Nagai. 2013. The effect of the sympathetic nervous system on splenic natural killer cell activity in mice administered the Lactobacillus pentosus strain S-PT84. *Neuro-report.* 24:988–991. <https://doi.org/10.1097/WNR.0000000000000036>
- Kaplan, M.H., Y.L. Sun, T. Hoey, and M.J. Grusby. 1996. Impaired IL-12 responses and enhanced development of Th2 cells in Stat4-deficient mice. *Nature.* 382:174–177. <https://doi.org/10.1038/382174a0>
- Klose, C.S., and D. Artis. 2019. Neuronal regulation of innate lymphoid cells. *Curr. Opin. Immunol.* 56:94–99. <https://doi.org/10.1016/j.coi.2018.11.002>
- Klose, C.S.N., T. Mahlaköiv, J.B. Moeller, L.C. Rankin, A.L. Flamar, H. Kabata, L.A. Monticelli, S. Moriyama, G.G. Putzel, N. Rakhilin, et al. 2017. The neuro-peptide neuromedin U stimulates innate lymphoid cells and type 2 inflammation. *Nature.* 549:282–286. <https://doi.org/10.1038/nature23676>
- Lanier, L.L. 2008. Up on the tightrope: natural killer cell activation and inhibition. *Nat. Immunol.* 9:495–502. <https://doi.org/10.1038/ni1581>
- Lau, C.M., and J.C. Sun. 2018. The widening spectrum of immunological memory. *Curr. Opin. Immunol.* 54:42–49. <https://doi.org/10.1016/j.coi.2018.05.013>
- Lau, C.M., N.M. Adams, C.D. Geary, O.E. Weizman, M. Rapp, Y. Pritykin, C.S. Leslie, and J.C. Sun. 2018. Epigenetic control of innate and adaptive immune memory. *Nat. Immunol.* 19:963–972. <https://doi.org/10.1038/s41590-018-0176-1>
- Liu, Q., W.N. Jin, Y. Liu, K. Shi, H. Sun, F. Zhang, C. Zhang, R.J. Gonzales, K.N. Sheth, A. La Cava, and F.D. Shi. 2017. Brain Ischemia Suppresses Immunity in the Periphery and Brain via Different Neurogenic Innervations. *Immunity.* 46:474–487. <https://doi.org/10.1016/j.immuni.2017.02.015>
- Loeper, M.C.O. 1904. L'action de l'adrénaline sur la sang. *Arch. Med. Exp. Anat. Pathol.* 16:83–108.
- Lopez-Vergès, S., J.M. Milush, B.S. Schwartz, M.J. Pando, J. Jarjoura, V.A. York, J.P. Houchins, S. Miller, S.M. Kang, P.J. Norris, et al. 2011. Expansion of a unique CD57⁺NKG2Chi natural killer cell subset during acute human cytomegalovirus infection. *Proc. Natl. Acad. Sci. USA.* 108: 14725–14732. <https://doi.org/10.1073/pnas.1110900108>
- Madera, S., and J.C. Sun. 2015. Cutting edge: stage-specific requirement of IL-18 for antiviral NK cell expansion. *J. Immunol.* 194:1408–1412. <https://doi.org/10.4049/jimmunol.1402001>
- Madera, S., M. Rapp, M.A. Firth, J.N. Beilke, L.L. Lanier, and J.C. Sun. 2016. Type I IFN promotes NK cell expansion during viral infection by protecting NK cells against fratricide. *J. Exp. Med.* 213:225–233. <https://doi.org/10.1084/jem.20150712>
- Meraz, M.A., J.M. White, K.C. Sheehan, E.A. Bach, S.J. Rodig, A.S. Dighe, D.H. Kaplan, J.K. Riley, A.C. Greenlund, D. Campbell, et al. 1996. Targeted disruption of the Stat1 gene in mice reveals unexpected physiologic specificity in the JAK-STAT signaling pathway. *Cell.* 84:431–442. [https://doi.org/10.1016/S0092-8674\(00\)81288-X](https://doi.org/10.1016/S0092-8674(00)81288-X)
- Moriyama, S., J.R. Brestoff, A.L. Flamar, J.B. Moeller, C.S.N. Klose, L.C. Rankin, N.A. Yudanin, L.A. Monticelli, G.G. Putzel, H.R. Rodewald, and D. Artis. 2018. β_2 -adrenergic receptor-mediated negative regulation of group 2 innate lymphoid cell responses. *Science.* 359:1056–1061. <https://doi.org/10.1126/science.aan4829>
- Murray, K., D.R. Godinez, I. Brust-Mascher, E.N. Miller, M.G. Gareau, and C. Reardon. 2017. Neuroanatomy of the spleen: Mapping the relationship between sympathetic neurons and lymphocytes. *PLoS One.* 12:e0182416. <https://doi.org/10.1371/journal.pone.0182416>
- Narni-Mancinelli, E., J. Chaix, A. Fenis, Y.M. Kerdiles, N. Yessaad, A. Reyniers, C. Gregoire, H. Luche, S. Ugolini, E. Tomasello, et al. 2011. Fate mapping analysis of lymphoid cells expressing the Nkp46 cell surface receptor. *Proc. Natl. Acad. Sci. USA.* 108:18324–18329. <https://doi.org/10.1073/pnas.1112064108>
- O'Sullivan, T.E., J.C. Sun, and L.L. Lanier. 2015. Natural Killer Cell Memory. *Immunity.* 43:634–645. <https://doi.org/10.1016/j.immuni.2015.09.013>
- Pedersen, L., M. Idorn, G.H. Olofsson, B. Lauenborg, I. Nookaew, R.H. Hansen, H.H. Johannesen, J.C. Becker, K.S. Pedersen, C. Dethlefsen, et al. 2016. Voluntary Running Suppresses Tumor Growth through Epinephrine- and IL-6-Dependent NK Cell Mobilization and Redistribution. *Cell Metab.* 23:554–562. <https://doi.org/10.1016/j.cmet.2016.01.011>
- Prass, K., C. Meisel, C. Höflich, J. Braun, E. Halle, T. Wolf, K. Ruscher, I.V. Victorov, J. Priller, U. Dirnagl, et al. 2003. Stroke-induced immunodeficiency promotes spontaneous bacterial infections and is mediated by sympathetic activation reversal by poststroke T helper cell type 1-like immunostimulation. *J. Exp. Med.* 198:725–736. <https://doi.org/10.1084/jem.20021098>
- Quatrini, L., E. Wieduwild, S. Guia, C. Bernat, N. Glaichenhaus, E. Vivier, and S. Ugolini. 2017. Host resistance to endotoxic shock requires the neuroendocrine regulation of group 1 innate lymphoid cells. *J. Exp. Med.* 214: 3531–3541. <https://doi.org/10.1084/jem.20171048>
- Quatrini, L., E. Vivier, and S. Ugolini. 2018a. Neuroendocrine regulation of innate lymphoid cells. *Immunol. Rev.* 286:120–136. <https://doi.org/10.1111/imr.12707>
- Quatrini, L., E. Wieduwild, B. Escaliere, J. Filtjens, L. Chasson, C. Laprie, E. Vivier, and S. Ugolini. 2018b. Endogenous glucocorticoids control host resistance to viral infection through the tissue-specific regulation of PD-1 expression on NK cells. *Nat. Immunol.* 19:954–962. <https://doi.org/10.1038/s41590-018-0185-0>
- Rapp, M., C.M. Lau, N.M. Adams, O.E. Weizman, T.E. O'Sullivan, C.D. Geary, and J.C. Sun. 2017. Core-binding factor β and Runx transcription factors promote adaptive natural killer cell responses. *Sci. Immunol.* 2: eaan3796. <https://doi.org/10.1126/sciimmunol.aan3796>
- Reeves, R.K., H. Li, S. Jost, E. Blass, H. Li, J.L. Schafer, V. Varner, C. Manickam, L. Eslamizar, M. Altfeld, et al. 2015. Antigen-specific NK cell memory in rhesus macaques. *Nat. Immunol.* 16:927–932. <https://doi.org/10.1038/ni.3227>
- Rosas-Ballina, M., M. Ochani, W.R. Parrish, K. Ochani, Y.T. Harris, J.M. Huston, S. Chavan, and K.J. Tracey. 2008. Splenic nerve is required for cholinergic antiinflammatory pathway control of TNF in endotoxemia. *Proc. Natl. Acad. Sci. USA.* 105:11008–11013. <https://doi.org/10.1073/pnas.0803237105>
- Santos-Rosa, H., R. Schneider, A.J. Bannister, J. Sherriff, B.E. Bernstein, N.C. Emre, S.L. Schreiber, J. Mellor, and T. Kouzarides. 2002. Active genes are tri-methylated at K4 of histone H3. *Nature.* 419:407–411. <https://doi.org/10.1038/nature01800>
- Staedtke, V., R.Y. Bai, K. Kim, M. Darvas, M.L. Davila, G.J. Riggins, P.B. Rothman, N. Papadopoulos, K.W. Kinzler, B. Vogelstein, and S. Zhou. 2018. Disruption of a self-amplifying catecholamine loop reduces cytokine release syndrome. *Nature.* 564:273–277. <https://doi.org/10.1038/s41586-018-0774-y>
- Sun, J.C., and L.L. Lanier. 2011. NK cell development, homeostasis and function: parallels with CD8⁺ T cells. *Nat. Rev. Immunol.* 11:645–657. <https://doi.org/10.1038/nri3044>
- Sun, J.C., J.N. Beilke, and L.L. Lanier. 2009. Adaptive immune features of natural killer cells. *Nature.* 457:557–561. <https://doi.org/10.1038/nature07665>

- Sun, J.C., S. Madera, N.A. Bezman, J.N. Beilke, M.H. Kaplan, and L.L. Lanier. 2012. Proinflammatory cytokine signaling required for the generation of natural killer cell memory. *J. Exp. Med.* 209:947–954. <https://doi.org/10.1084/jem.20111760>
- Tarr, A.J., N.D. Powell, B.F. Reader, N.S. Bhawe, A.L. Roloson, W.E. Carson III, and J.F. Sheridan. 2012. β -Adrenergic receptor mediated increases in activation and function of natural killer cells following repeated social disruption. *Brain Behav. Immun.* 26:1226–1238. <https://doi.org/10.1016/j.bbi.2012.07.002>
- Vivier, E., D.H. Raulet, A. Moretta, M.A. Caligiuri, L. Zitvogel, L.L. Lanier, W.M. Yokoyama, and S. Ugolini. 2011. Innate or adaptive immunity? The example of natural killer cells. *Science.* 331:44–49. <https://doi.org/10.1126/science.1198687>
- Wallrapp, A., S.J. Riesenfeld, P.R. Burkett, R.E. Abdunour, J. Nyman, D. Dionne, M. Hofree, M.S. Cuoco, C. Rodman, D. Farouq, et al. 2017. The neuropeptide NMU amplifies ILC2-driven allergic lung inflammation. *Nature.* 549:351–356. <https://doi.org/10.1038/nature24029>
- Wieduwild, E., M. Girard-Madoux, L. Quatrini, C. Laprie, L. Chasson, R. Rossignol, C. Bernat, S. Guia, and S. Ugolini. 2020. β 2-adrenergic signals downregulate the innate immune response and reduce host resistance to viral infection. *J. Exp. Med.* <https://doi.org/10.1084/jem.20190554>
- Yokoyama, W.M., S. Kim, and A.R. French. 2004. The dynamic life of natural killer cells. *Annu. Rev. Immunol.* 22:405–429. <https://doi.org/10.1146/annurev.immunol.22.012703.104711>

Supplemental material

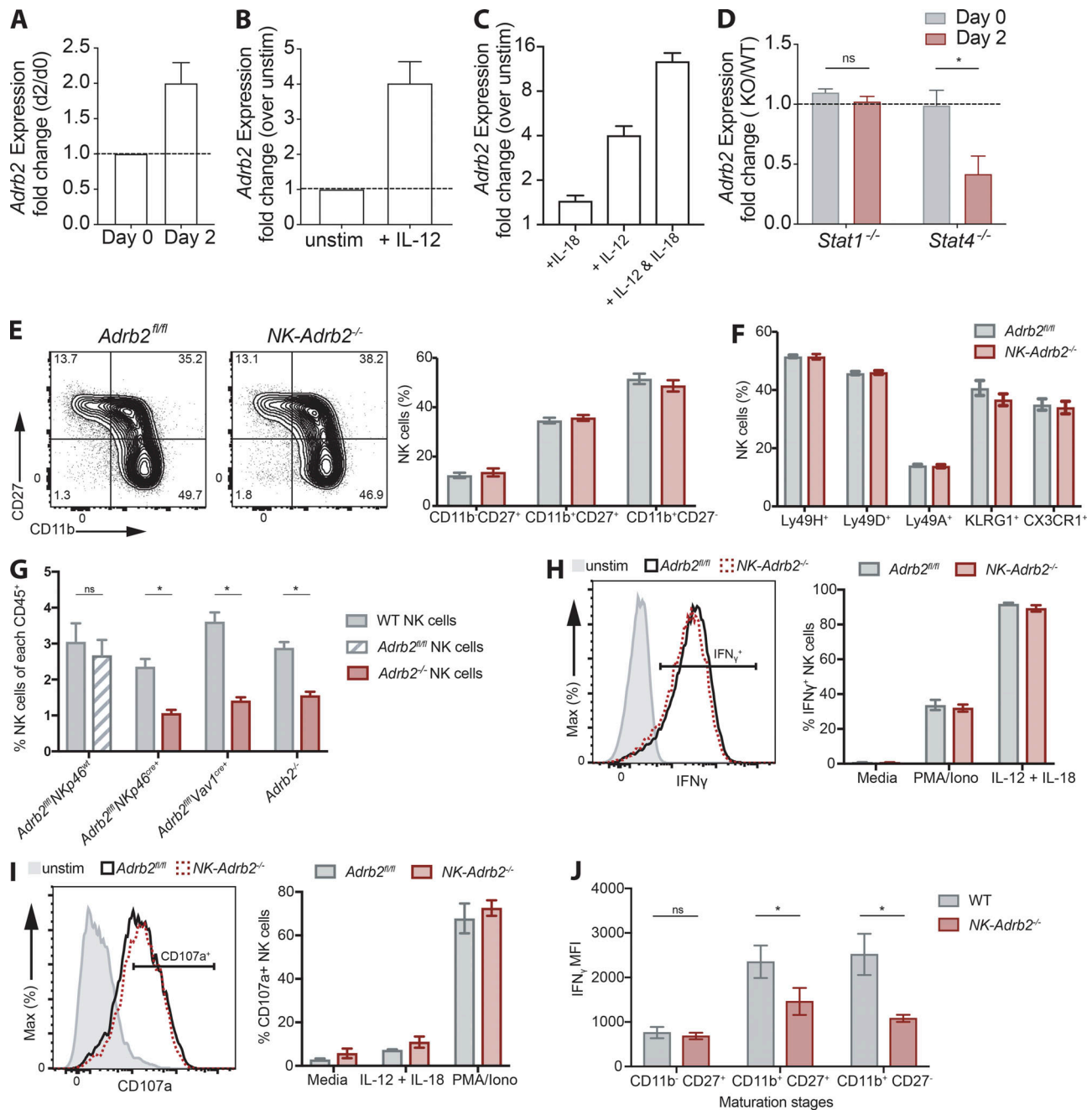


Figure S1. *Adrb2* is dispensable for NK cell effector function in vitro and maturation in a noncompetitive setting. Related to Figs. 2 and 3. **(A)** Real-time PCR analysis of *Adrb2* mRNA in WT NK cells sorted at steady-state or day 2 PI ($n = 3$ samples per condition). **(B and C)** Real-time PCR analysis of *Adrb2* mRNA in WT NK cells stimulated with IL-12 or left unstimulated (B), or stimulated with a combination of IL-12 and/or IL-18 (C) normalized to mRNA levels in unstimulated NK cells ($n = 3$ samples per condition). **(D)** Real-time PCR analysis of *Adrb2* mRNA in *Stat*-deficient Ly49H⁺ NK cells sorted at steady-state or day 2 PI from WT: *Stat1*^{-/-} and WT: *Stat4*^{-/-} mBMCs, normalized to mRNA levels in WT Ly49H⁺ NK cells at each time point ($n = 2$ or 3 mice per group). **(E)** Representative flow plots showing the expression of maturation markers CD11b and CD27 NK cells from *NK-Adrb2*^{-/-} or littermate *Adrb2*^{fl/fl} mice at steady-state. Graph shows the quantification of the percentage of NK cells expressing these markers. Representative of three independent experiments with five mice per group. **(F)** Percentage of circulating NK cells expressing various activating (Ly49H, Ly49D) and inhibitory (Ly49A) receptors, and markers of terminal maturation (KLRG1, CX3CR1) at steady-state. Representative of two independent experiments with four to six mice per group. **(G)** Quantification of circulating NK cells (NK1.1⁺ CD49b⁺ Lin⁻) as percentage of total CD45⁺ cells in mixed WT(CD45.1): *Adrb2*-deficient (CD45.2) mBMC mice at steady-state, generated using the genetic mouse models indicated, or WT(CD45.1): *Adrb2*^{fl/fl} littermate (CD45.2) mBMCs. Representative of two independent experiments with at least five mice per group. Statistical differences ($P < 0.05$) were calculated using Sidak's multiple comparisons test (two-way ANOVA) and indicated with a single star (*). **(H and I)** Representative histogram of the percentage of splenic NK cells from *NK-Adrb2*^{-/-} or littermate *Adrb2*^{fl/fl} mice producing IFN- γ (H) or degranulating (I) after 4 h ex vivo stimulation with IL-12 and IL-18 or PMA and ionomycin, respectively. Representative of two independent experiments with two samples per condition. **(J)** Quantification of the production of IFN- γ (shown as MFI) by *Adrb2*^{-/-} and WT NK cells at each maturation stage 2 d following MCMV infection in a mBMC setting. Representative of two independent experiments with four mice per group. Statistical differences ($P < 0.05$) were calculated using Sidak's multiple comparisons test (two-way ANOVA) and indicated with a single star (*). Iono, ionomycin. All bar plots show mean \pm SEM.

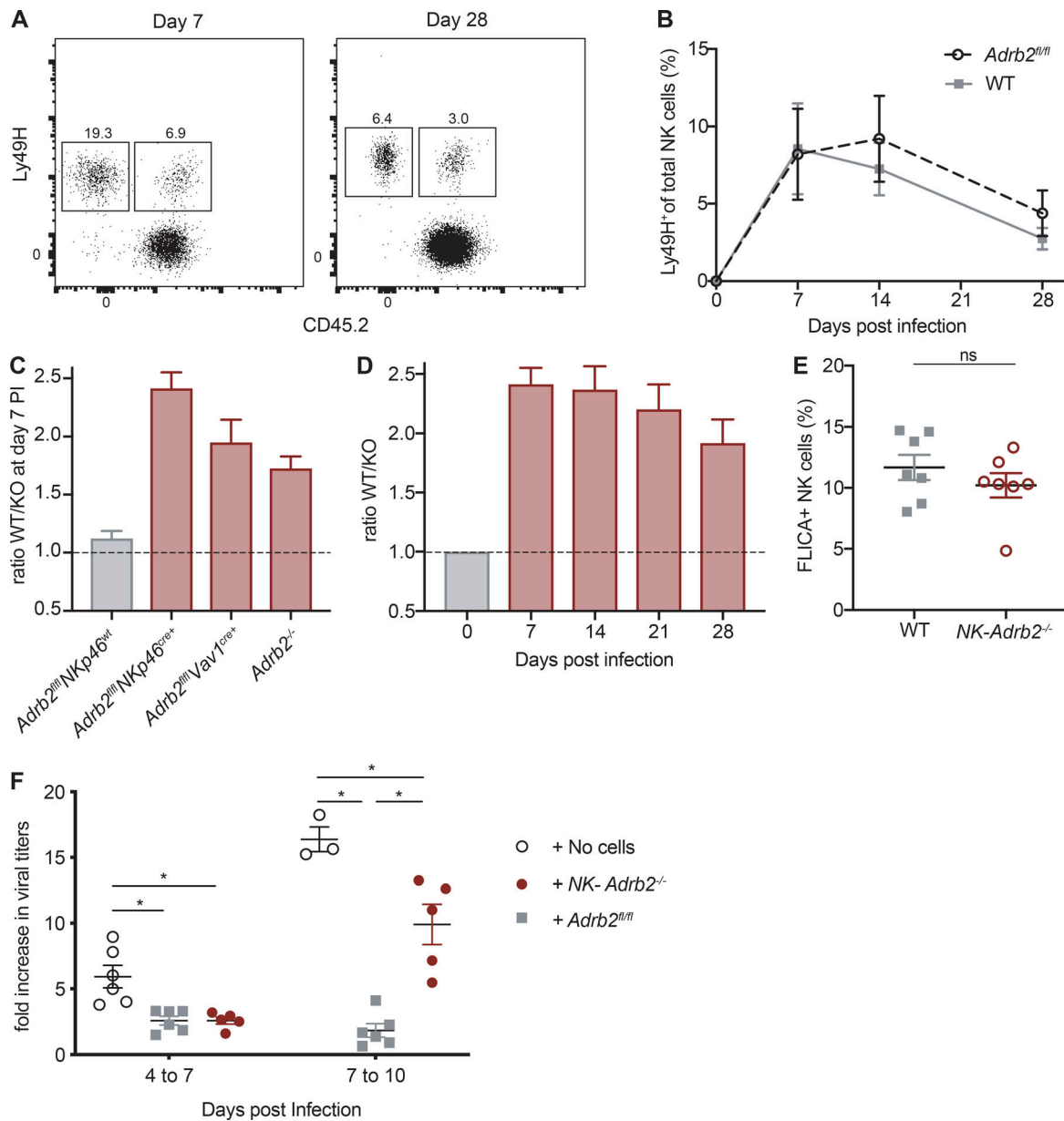


Figure S2. **β 2AR is required for NK cell expansion but not memory maintenance.** Related to Figs. 4 and 5. **(A)** Representative flow plots showing the percentages of transferred WT and *NK-Adrb2^{-/-}* Ly49H⁺ NK cells of total circulating NK cells at day 7 and 28 PI. **(B)** The percentage of transferred WT and littermate *Adrb2^{fl/fl}* Ly49H⁺ NK cells was quantified in peripheral blood as indicated. Data are pooled from two independent experiments with four or five mice per group. **(C)** The ratio of transferred WT and *Adrb2*-deficient Ly49H⁺ NK cells from the indicated genetic mouse models, or littermate *Adrb2^{fl/fl}* controls, was calculated in peripheral blood at day 7 PI. Representative of two independent experiments with five mice per group. **(D)** The ratio of transferred WT and *NK-Adrb2^{-/-}* Ly49H⁺ NK cells was quantified in peripheral blood weekly as indicated. Representative of three independent experiments with five mice per group. **(E)** As in Fig. 4 C. The percentage of apoptotic WT and *NK-Adrb2^{-/-}* Ly49H⁺ NK cells (as detected by FLICA stain, marking active caspases in live cells) was measured at day 4 PI. Data are representative of two independent experiments with four mice per group. **(F)** As in Fig. 5 D. The viral replication rate for each mouse is presented as fold increase in viral titers between each two consequent time points. Statistical differences ($P < 0.05$) were calculated using Sidak's multiple comparisons test (two-way ANOVA) and indicated with a single star (*). All bar plots show mean \pm SEM.